

# Soil Classification Using Mid-Infrared Off-Normal Active Differential Reflectance Characteristics

Ram M. Narayanan, Steven E. Green, and Dennis R. Alexander  
Center for Electro-Optics, University of Nebraska, Lincoln, NE 68588

**ABSTRACT:** Active mid-infrared laser reflectance characteristics of 18 different bench-mark soil samples were measured at various angles of incidence between 0° and 80° at 9.283-, 9.569-, 10.247-, and 10.633- $\mu\text{m}$  wavelengths for both co-polarized and cross-polarized conditions. Calibration was performed for each measurement using a Labsphere Infragold diffuse reflectance standard of 94 percent reflectance. One hundred independent reflectivity measurements were averaged for each combination to yield a mean reflectance value. The soil samples were characterized in terms of the soil taxonomy, mineralogy, geographic location, soil texture, and organic carbon content. Selected samples represented wide variability in soil properties.

Measurements indicate that these soils have unique reflectance signatures in the 9- to 11- $\mu\text{m}$  mid-infrared region. On the basis of the data, we present an algorithm using off-normal co-polarized reflectance ratios at various wavelengths, to uniquely identify all 18 soils investigated. We show from theoretical considerations and experimental observations that the reflectance ratios are more insensitive to variations in incidence angle at angles off-normal compared to near-normal incidence.

## INTRODUCTION

LASER REMOTE SENSING HAS POTENTIAL WIDESPREAD APPLICATIONS in a variety of meteorological, geophysical, and oceanographic measurements. The study of mid-infrared reflectance of natural surface materials has been motivated from two main applications; viz., (i) remote sensing of terrestrial lithology (Eberhardt *et al.*, 1985), and (ii) calibration of downward-looking DIAL pollution sensors (Shumate *et al.*, 1982).

Laser reflectance measurements of a variety of benchmark soil samples were made at different wavelengths (9.283, 9.569, 10.247, and 10.633  $\mu\text{m}$ ), incidence angles (0°, 20°, 40°, 60°, and 80°) and polarizations (co- and cross-polarized). Incidence angle refers to the angle between the mean surface normal and the incident ray. In order to provide a unique and comprehensive database for various applications, soil samples were chosen to exhibit wide variability in their physical properties and geographical location within the United States.

Our measurements indicate that the reflectance characteristics of soils versus wavelength show differences in the 9- to 11- $\mu\text{m}$  wavelength region. Thus, these differences can be exploited in identifying and discriminating various types of soils using reflectance ratios at different wavelengths. Such a differential reflectance scheme has been proposed in the past using reflectances at near-normal incidence (Cvijin *et al.*, 1987). The next section describes briefly the test setup, description of soils studied, and reflectance characteristics measured. Then, a theoretical justification is presented for using reflectance ratios at incidence angles off-normal, which is more tolerant of wide variations in incidence angle. A classification algorithm, based on the off-normal reflectance ratios at different wavelengths is presented in the fourth section, which can be used as a basis for remote identification and discrimination of various soil types. Conclusions are discussed in the final section.

## REFLECTANCE CHARACTERISTICS

### TEST SETUP

The experimental setup is shown in Figure 1. The source of radiation used was a coherent 100 W CO<sub>2</sub> laser, line tunable to 53 lines over the 9- to 11- $\mu\text{m}$  wavelength range. However, the

laser was operated at 5 W for our measurements. The continuous laser beam was chopped at 2 kHz rate to generate pulsed signals which were then incident on a sample of the soil material placed in a petri dish on a rotating turntable. The soils were dried, poured, and leveled on the petri dish, prior to making the reflectance measurements. As the turntable rotated, the laser beam pulses were scattered from different portions of the target material, so that the average backscatter could be computed. A 24-cm focal length lens was used to image the target surface onto a Cryostat-cooled HgCdTe infrared detector. A 10,000:1 extinction ratio polarizer in front of the detector was used to select backscattered radiation with polarization either parallel (copolarized) or perpendicular (cross-polarized) to that of the illuminating beam. The detector output was amplified in a matched preamplifier prior to recording.

One hundred independent reflectivity measurements were averaged to reduce the effects of intensity fluctuations due to speckle. Speckle refers to the random intensity distribution that occurs when coherent light is reflected from rough surfaces (Dainty, 1984). In addition, each of the 100 recorded measurements was essentially an average of approximately 500 speckle values, obtained by dividing the time for each measurement (250 milliseconds) by the interpulse duration (0.5 milliseconds). Thus, a total of 50,000 independent samples were, in fact, averaged to yield the mean reflectance value. We therefore estimate the relative accuracy ( $\pm 1$  standard deviation) of our data obtained to be better than  $\pm 0.5$  percent. Measurement repeatability for five replicates was determined to be  $\pm 2.8$  percent for co-polarized and  $\pm 8.3$  percent for cross-polarized data. For calibration, a Labsphere Infragold diffuse reflectance standard of mean reflectance  $0.944 \pm 0.036$  (Willey, 1987) was used.

### SOILS DESCRIPTION

Mid-infrared reflectance characteristics of 18 different soils were studied (Narayanan *et al.*, 1990), whose major characteristics are summarized in Table 1. As is evident from the table, the soils show wide variability in their physical properties and represent typical soils found within the United States. Brief descriptions of the soils, as given in Donahue *et al.* (1983), are given below.

*Mollisols* are dark-colored, mainly organic, soils of grasslands



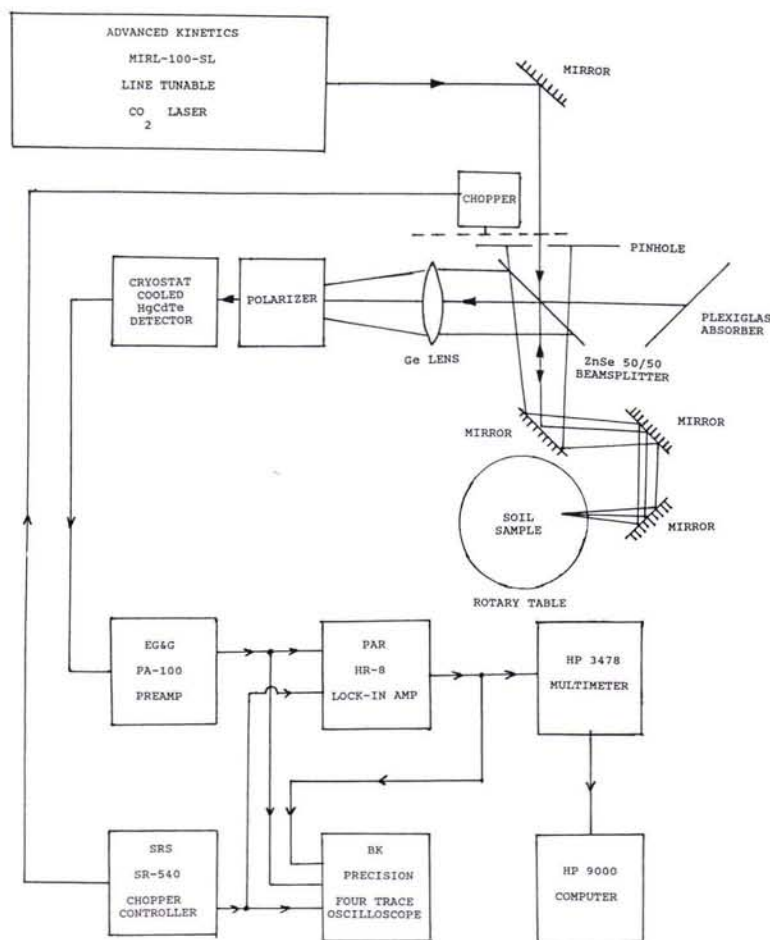


FIG. 1. Block diagram of experimental apparatus.

and some hardwood forests with high basic cation supply. *Alfisols* are high-percentage basic cation-saturated soils in areas of sufficient precipitation, that move enough clay downward to form a clay accumulation layer. *Ustisols* are humid-area soils, low in basic cation-saturation, but not as weathered as *oxisols*. *Aridisols* are arid-area soils characterized by well developed pedogenic horizons, low soil moisture, and low organic matter. *Entisols* are soils of slight development, with no significant horizon development, while *vertisols* are developed from high-limestone parent materials, and have high clay contents. *Spodosols* are well leached, having low basic cation-saturation and possess moderate to strong acidic sandy profiles. *Oxisols* are intensely weathered soils which have lost much of their silica, and are rich in  $Fe_2O_3$  and  $Al_2O_3$ . These soils occur in hot/humid hardwood forest areas. *Inceptisols* are weakly developed soils showing wide variability in profiles.

For a more detailed explanation of the characteristics of various soil types, the reader is referred to Buol *et al.* (1989).

#### REFLECTANCE CHARACTERISTICS

Most soils exhibited reflectance values that decreased as the wavelength of illumination increased. This phenomenon is attributed to the presence of quartz that exhibits a reststrahlen band near  $9 \mu m$ . A notable exception is soil 18, which shows a peak in the reflectance structure at  $9.569 \mu m$ , possibly because of its kaolinitic mineralogy. Our X-ray diffraction analysis indicates that soil 18 contains well-crystallized kaolinite. Previous studies indicate that the reflectance spectrum of well-crystallized pure kaolinite exhibits a reststrahlen band around  $9.35$  to

$9.45 \mu m$  (Salisbury *et al.*, 1987; Cvijin *et al.*, 1987). While the Salisbury *et al.* (1987) data show that higher laser reflectance can be expected at  $9.283 \mu m$  compared to  $9.569 \mu m$ , the Cvijin *et al.* (1987) data indicate just the opposite. Our measurements are consistent with the data acquired by Cvijin *et al.* (1987). Also of interest is the reflectance characteristic of soil 17, which shows generally lower reflectance values (about 25 to 30 percent) compared to the other soils investigated.

Figures 2 through 5 show co-polarized reflectances versus wavelength at various incidence angles ( $A=0^\circ$ ,  $B=20^\circ$ ,  $C=40^\circ$ ,  $D=60^\circ$ , and  $E=80^\circ$ ) for soils 04, 09, 18, and 17. The  $y$ -axis in the above plots is the normalized reflectance value, i.e., the ratio of the power reflected from the target at the specified incidence angle and polarization to the co-polarized power reflected from the reference standard at  $0^\circ$  incidence. These figures provide an indication of the wide variability that exists in the mid-infrared reflectance characteristics of typical soils.

#### THEORETICAL CONSIDERATIONS

Various theoretical models can be applied to the scattering of optical radiation from rough soil surfaces. A two-scale roughness analytical model, modified to account for shadowing due to macrostructures, has been found to yield good agreement with measured bidirectional reflectivity of various soils (Becker *et al.*, 1985). In this section, simpler scattering models are considered for randomly rough surfaces to study the factors affecting the reflectance ratios at different wavelengths as a function of incidence angle, and to compare the model predictions with measurements.

TABLE 1. SUMMARY OF CLASSIFICATION, SAMPLE LOCATION, AND TEXTURE FOR BENCHMARK SOILS

| Soil # | Soil Order | Great or subgroup    | Series        | Mineralogy*       | Location       | Horizon | Clay    | Silt    | Organic |
|--------|------------|----------------------|---------------|-------------------|----------------|---------|---------|---------|---------|
|        |            |                      |               |                   |                |         | Content | Content | Carbon  |
|        |            |                      |               |                   |                |         | %       | %       | %       |
| 01     | Mollisol   | Typic Haploxerall    | Walla Walla   | Q,P,K-sp,H/M,U    | Oregon         | A       | 18      | 67      | 1.09    |
| 02     | Mollisol   | Udic Haploboroll     | Barnes        | Q,P,U,Py          | North Dakota   | A       | 15      | 69      | 0.53    |
|        |            |                      |               |                   |                | B       | 26      | 36      | 2.17    |
| 03     | Mollisol   | Typic Hapludoll      | Clarion       | Q,P,H/M,S         | Iowa           | A       | 28      | 36      | 0.96    |
|        |            |                      |               |                   |                | B       | 21      | 28      | 1.31    |
| 04     | Mollisol   | Torrertic Paleustoll | Pullman       | Q,P,K-sp,U,A      | Texas          | A       | 22      | 30      | 0.83    |
|        |            |                      |               |                   |                | B       | 34      | 51      | 0.92    |
| 05     | Mollisol   | Typic Arguidoll      | Sharpsburg    | Q,P,K-sp,H/M,U    | Nebraska       | A       | 43      | 44      | 0.71    |
|        |            |                      |               |                   |                | B       | 36      | 62      | 1.69    |
| 06     | Alfisol    | Typic Paleudalf      | Crider        | Q,P,K-sp,H/M,U    | Kentucky       | A       | 38      | 60      | 1.03    |
|        |            |                      |               |                   |                | B       | 25      | 73      | 2.14    |
| 07     | Alfisol    | Typic Hapludalf      | Miami         | Q,P,K-sp,H/M,U    | Indiana        | A       | 34      | 64      | 0.33    |
|        |            |                      |               |                   |                | B       | 22      | 50      | 1.23    |
| 08     | Alfisol    | Typic Xerorthent     | Yolo          | Q,P,K-sp,H/M,U    | California     | A       | 34      | 34      | 0.58    |
|        |            |                      |               |                   |                | B       | 26      | 54      | 1.31    |
| 09     | Ultisol    | Typic Paleudult      | Frederick     | Q,K-sp,K          | Virginia       | A       | 26      | 54      | 0.86    |
|        |            |                      |               |                   |                | B       | 19      | 62      | 2.19    |
| 10     | Ultisol    | Typic Hapludult      | Cecil         | Q,P,H/M,K,S       | North Carolina | A       | 37      | 51      | 0.25    |
|        |            |                      |               |                   |                | B       | 10      | 20      | 3.20    |
| 11     | Ultisol    | Typic Paleaquult     | Rains         | Q,P,K-sp,H/M,K,G? | South Carolina | A       | 51      | 17      | 0.28    |
|        |            |                      |               |                   |                | B       | 17      | 50      | 3.40    |
| 12     | Aridisol   | Typic Haplargid      | Mohave        | Q,K-sp,H/M,C,S    | Arizona        | A       | 27      | 56      | 0.82    |
|        |            |                      |               |                   |                | B       | 26      | 24      | 0.67    |
| 13     | Aridisol   | Ustollic Haplargid   | Fort Collins  | Q,P,H/M,C,U       | Colorado       | A       | 19      | 17      | 0.25    |
|        |            |                      |               |                   |                | B       | 29      | 17      | 0.77    |
| 14     | Entisol    | Typic Ustipsamment   | Valentine     | Q,P,K-sp,H/M,U    | Nebraska       | A       | 30      | 19      | 0.53    |
|        |            |                      |               |                   |                | B       | 06      | 05      | 0.81    |
| 15     | Vertisol   | Udic Pellustert      | Houston Black | Q,P,H/M,U         | Texas          | A       | 04      | 02      | 0.41    |
|        |            |                      |               |                   |                | B       | 48      | 40      | 1.61    |
| 16     | Spodosol   | Dystril Eutrochrept  | Caribou       | Q,P,K-sp,H/M,K,U  | Maine          | A       | 58      | 36      | 1.04    |
|        |            |                      |               |                   |                | B       | 14      | 46      | 2.37    |
| 17     | Oxisol     | Ustoxic Humitrop     | Kole Kole     | Q,H/M,K,U         | Hawaii         | A       | 14      | 42      | 1.52    |
|        |            |                      |               |                   |                | B       | 14      | 38      | 3.46    |
| 18     | Inceptisol | Tropeptic Eutrustox  | Wahiawa       | H,K               | Hawaii         | A       | 60      | 33      | 1.30    |

\*Q=quartz, P=plagioclase feldspar, K-sp=potassium feldspar, H/M=hematite and/or magnetite, C=calcite, K=kaolinite, S=smectite, U=unspecified clay, Py=pyrolusite, A=apatite, G=gibbsite.

The co-polarized backscattering coefficient for a Gaussian distributed random rough surface can be separated into a specular or coherent component  $\sigma_c^\circ$ , and a diffuse or incoherent component  $\sigma_n^\circ$  (Fung, 1982). Although the analysis is valid for a Gaussian surface height model, the results should be applicable to other surface models also. For a slightly rough surface, coherent scattering is significant near the specular direction (normal incidence for backscatter), while incoherent scattering is important in off-specular directions (Clay *et al.*, 1973; Fung, 1984). Soil surfaces typically have small-scale surface roughness,  $\sigma$ , of the order of the mean particle size, which is approximately 1 to 5  $\mu\text{m}$ ; thus  $k\sigma$ , where  $k = \frac{2\pi}{\lambda} \sim 0.6 \mu\text{m}^{-1}$ , is approximately 0.6 to 3.0 in our case. It may also be noted that the best fit of a two-scale surface scattering model to measured data at 10.6  $\mu\text{m}$  was obtained for a roughness value of about 1  $\mu\text{m}$  (Becker *et al.*, 1985). The surfaces can therefore be characterized as slightly rough to medium rough (Fung, 1984).

The co-polarized reflectance ratio,  $P_{ij}$ , is given by

$$P_{ij} = \frac{\sigma^\circ(\lambda_i)}{\sigma^\circ(\lambda_j)} \quad (1)$$

where  $\sigma^\circ$  is the co-polarized backscatter cross-section per unit area, and  $\lambda_i$  and  $\lambda_j$  are the wavelengths considered. The cross-

section per unit area is proportional to the power reflected by a flood-illuminated sample of the target material (Leader, 1979). At near-normal incidence,  $\sigma^\circ \approx \sigma_c^\circ$ , the coherent component, which is given by (Fung, 1982)

$$\sigma_c^\circ(\lambda) = (2L)^2 C e^{-K} \text{sinc}^2(2kL \sin \theta) \quad (2)$$

where

$$C = \pi \left\{ \frac{k|R(0,\lambda)|\cos\theta}{\pi} \right\}^2, \text{ and}$$

$$K = 4k^2\sigma^2 \cos^2\theta.$$

In Equation 2,  $2L$  is the diameter of the illuminated patch,  $\sigma$  is the RMS surface roughness, and  $R(0,\lambda)$  is the reflection coefficient of the smooth soil surface at  $0^\circ$  incidence at wavelength  $\lambda$ .

$R(0,\lambda)$  is related to the relative permittivity  $\epsilon_r(\lambda)$  by

$$R(0,\lambda) = \frac{\sqrt{\epsilon_r(\lambda)} - 1}{\sqrt{\epsilon_r(\lambda)} + 1}$$

At small angles of incidence, the term  $2kL \sin \theta$  is small, and



REFLECTANCE VS WAVELENGTH

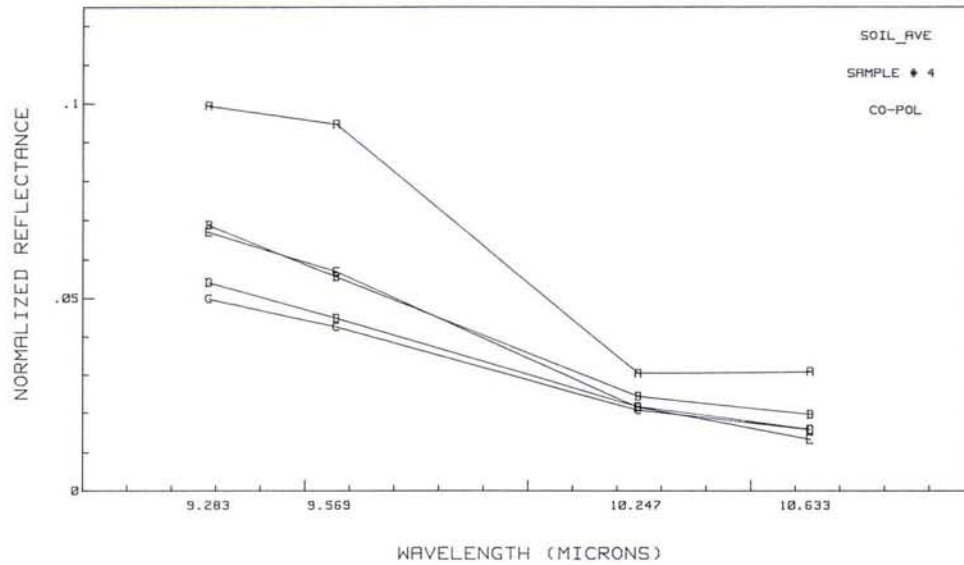


FIG. 2. Normalized co-polarized reflectance of soil 04 vs. wavelength at various angles of incidence. Incidence angles are A = 0°, B = 20°, C = 40°, D = 60°, and E = 80°.

REFLECTANCE VS WAVELENGTH

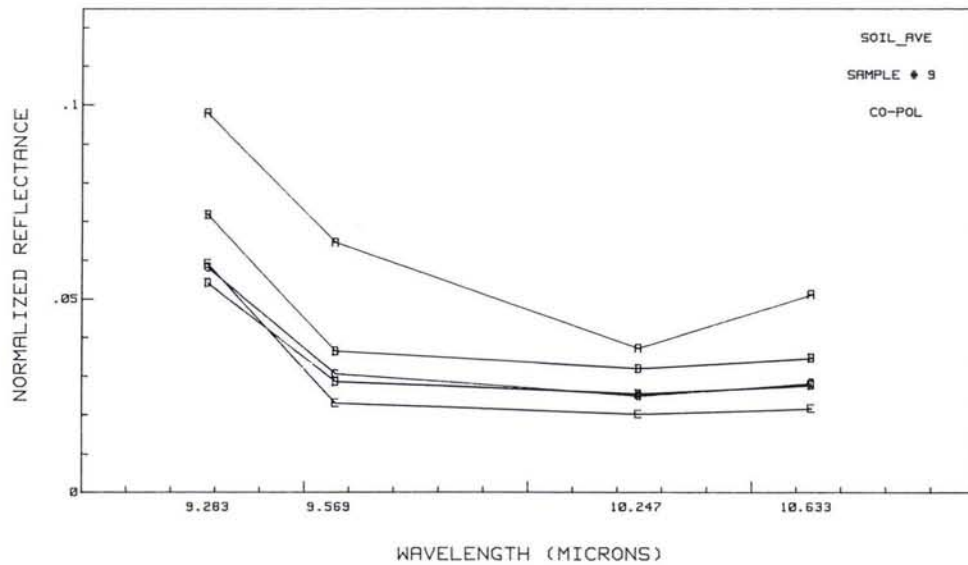


FIG. 3. Normalized co-polarized reflectance of soil 09 vs. wavelength at various angles of incidence. Incidence angles are A = 0°, B = 20°, C = 40°, D = 60°, and E = 80°.

the sinc-squared function is approximately equal to 1. Thus, we can simplify  $\sigma_c^\circ(\lambda)$  as

$$\sigma_c^\circ(\lambda) = 16\pi \left(\frac{L}{\lambda}\right)^2 |R(0, \lambda)|^2 \cos^2 \theta \exp \left\{ \frac{-16\pi^2 \sigma^2 \cos^2 \theta}{\lambda^2} \right\}. \quad (3)$$

Thus, for near-normal incidence,

$$P_{ij} = \left[ \frac{R(0, \lambda_i)}{R(0, \lambda_j)} \right]^2 \left( \frac{\lambda_j}{\lambda_i} \right)^2 \exp \left\{ -16\pi^2 \sigma^2 \cos^2 \theta \left[ \frac{1}{\lambda_i^2} - \frac{1}{\lambda_j^2} \right] \right\} \quad (4)$$

Therefore,  $dP_{ij}/d\theta$ , given by

$$\frac{dP_{ij}}{d\theta} = \left[ \frac{R(0, \lambda_i)}{R(0, \lambda_j)} \right]^2 \left( \frac{\lambda_j}{\lambda_i} \right)^2 16\pi^2 \sigma^2 \sin 2\theta \left[ \frac{1}{\lambda_i^2} - \frac{1}{\lambda_j^2} \right] \exp \left\{ -16\pi^2 \sigma^2 \cos^2 \theta \left[ \frac{1}{\lambda_i^2} - \frac{1}{\lambda_j^2} \right] \right\} \quad (5)$$

is a function of the incidence angle,  $\theta$ . This indicates that the reflectance ratio varies with the angle of incidence, which may not be a desirable feature in field applications.

At off-normal incidence angles, usually beyond 10°, the in-

REFLECTANCE VS WAVELENGTH

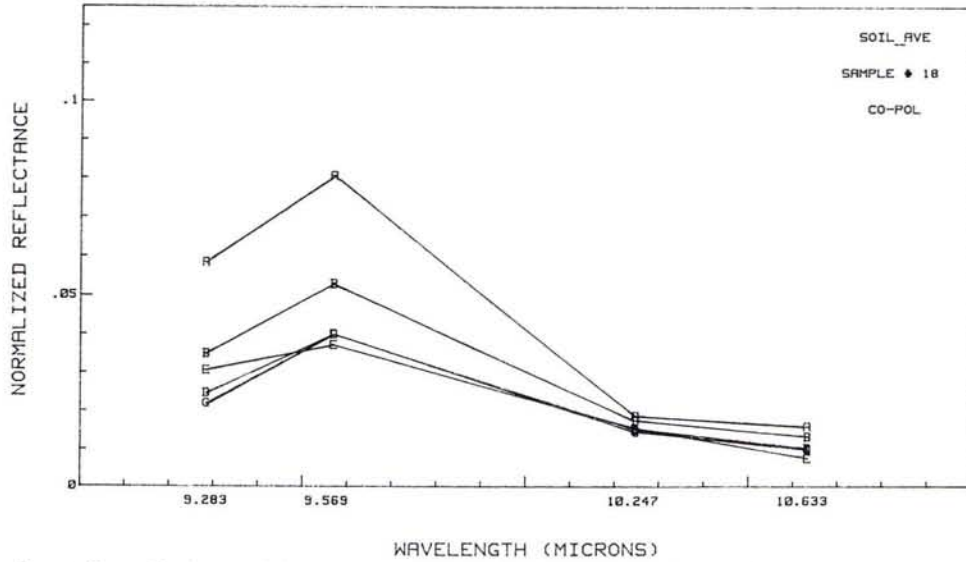


FIG. 4. Normalized co-polarized reflectance of soil 18 vs. wavelength at various angles of incidence. Incidence angles are A = 0°, B = 20°, C = 40°, D = 60°, and E = 80°.

REFLECTANCE VS WAVELENGTH

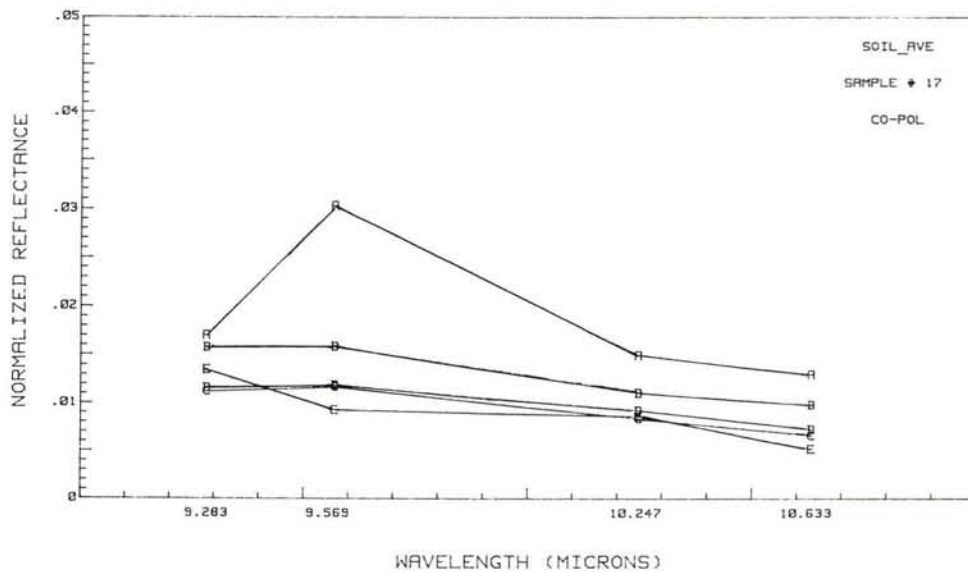


FIG. 5. Normalized co-polarized reflectance of soil 17 vs. wavelength at various angles of incidence. Incidence angles are A = 0°, B = 20°, C = 40°, D = 60°, and E = 80°.

coherent term dominates. This term is computed using the Kirchhoff model, and is given by Fung (1984) as

$$\sigma_n(\lambda) = \pi |R(0, \lambda)|^2 \sec^4 \theta p(\tan \theta)$$

where  $p(\tan \theta)$  is the probability density function of the surface slope.

Hence,  $P_{ij}$  can be written as

$$P_{ij} = \frac{|R(0, \lambda_i)|^2}{|R(0, \lambda_j)|^2} \quad (6)$$

which is independent of the incidence angle,  $\theta$ . Thus  $dP_{ij}/d\theta = 0$ .

The above analysis shows that the reflectance ratios should be more insensitive to variations in incidence angle under off-normal rather than near-normal conditions. This has also been verified experimentally for all 18 soils investigated. Table 2 presents the measured co-polarized  $P_{ij}$  ratios versus incidence angles for Soil 01, which are typical of the other soils in Table 1. We denote as  $P_1, P_2, P_3,$  and  $P_4$  the normalized co-polarized reflectance values at 9.283  $\mu\text{m}$ , 9.569  $\mu\text{m}$ , 10.247  $\mu\text{m}$ , and 10.633

TABLE 2.  $P_{ij}$  RATIOS OF SOIL 01

| $P_{ij}$ ratio | Incidence Angle |       |       |       |       |
|----------------|-----------------|-------|-------|-------|-------|
|                | 0°              | 20°   | 40°   | 60°   | 80°   |
| $P_{21}$       | 1.020           | 0.931 | 0.909 | 0.901 | 0.889 |
| $P_{31}$       | 0.392           | 0.581 | 0.548 | 0.549 | 0.562 |
| $P_{41}$       | 0.458           | 0.486 | 0.494 | 0.476 | 0.451 |
| $P_{32}$       | 0.384           | 0.625 | 0.604 | 0.607 | 0.632 |
| $P_{42}$       | 0.448           | 0.522 | 0.544 | 0.529 | 0.507 |
| $P_{43}$       | 1.167           | 0.837 | 0.902 | 0.871 | 0.803 |

$\mu_m$ , respectively. The following ratios are indicated:

$$\begin{aligned}
 P_{21} &= P_2/P_1, \\
 P_{31} &= P_3/P_1, \\
 P_{41} &= P_4/P_1, \\
 P_{32} &= P_3/P_2, \\
 P_{42} &= P_4/P_2, \text{ and} \\
 P_{43} &= P_4/P_3.
 \end{aligned}
 \tag{7}$$

As is evident from the table, the  $P_{ij}$  ratios are quite close to each other in the range of incidence angles from 20° to 80°, while corresponding values at 0° are quite different. Thus, from a remote sensing viewpoint, it is better to use off-normal reflectance ratios for soil identification and discrimination.

CLASSIFICATION ALGORITHM

An algorithm based on co-polarized reflectance ratios of various wavelengths investigated is presented that may be useful in identifying and classifying the soils studied. We denote as  $\bar{P}_{ij}$  the average off-normal reflectance ratio  $P_{ij}$ . Averaged ratios at 20°, 40°, and 60° incidence angle have been used. The value at 80° incidence is not used, because the Kirchhoff model may not be applicable at this incidence angle. For each sample, the following six average reflectance ratios are formed:  $\bar{P}_{21}$ ,  $\bar{P}_{31}$ ,  $\bar{P}_{41}$ ,  $\bar{P}_{32}$ ,  $\bar{P}_{42}$ , and  $\bar{P}_{43}$ . Table 3 shows the average reflectance ratios of all 18 soils investigated.

In order to use these reflectance ratios for soil discrimination, a statistical analysis is performed to determine the difference required between the  $\bar{P}_{ij}$  ratios of two different soils so as to be able to separate them at an acceptable confidence level.

One approach that was followed was to consider the probability density of  $\bar{P}_{ij} = \frac{A}{B}$  where  $A = \frac{1}{N} \sum_{k=1}^N \rho_{ik}$  and  $B = \frac{1}{N} \sum_{k=1}^N \rho_{jk}$  and  $\rho_{jk}$  refer to the  $k$ -th sample of the measured reflectance values at wavelengths  $\lambda_i$  and  $\lambda_j$ , respectively, and are proportional to the reflected or backscattered power; while  $N$  is the total number of samples averaged. Because the number of samples,  $N$ , is large, we can assume that the variables  $A$  and  $B$  are normally distributed with means  $\mu_A$  and  $\mu_B$ , respectively, and standard deviation  $\sigma_A$  and  $\sigma_B$ , respectively. This follows from the Central Limit Theorem. Because  $\bar{P}_{ij}$  is the ratio of two normally distributed random variables, it has a Cauchy density function centered at  $\mu_A/\mu_B$  (Papoulis, 1984). However, because the moments of the Cauchy density function are not defined (Abramowitz and Stegun, 1965), this approach was discarded.

An alternate approach, using propagation of errors or variances, yielded more meaningful results than the method considered above. Because  $\bar{P}_{ij} = \frac{A}{B}$ , we obtain (Taylor, 1982)

$$\left| \frac{d\bar{P}_{ij}}{\bar{P}_{ij}} \right| = \left| \frac{dA}{A} \right| + \left| \frac{dB}{B} \right|
 \tag{8}$$

where  $d\bar{P}_{ij}$ ,  $dA$ , and  $dB$  are the errors in  $\bar{P}_{ij}$ ,  $A$ , and  $B$ , respectively. Because our measurement precision is estimated as  $\pm 0.5$  percent, and repeatability was measured as  $\pm 2.8$  percent, the total error in  $A$  or  $B$  is computed as the sum of the above, i.e.,  $\pm 3.3$  percent. Thus, we have

$$\left| \frac{dA}{A} \right| = \left| \frac{dB}{B} \right| = 0.033$$

which yields

$$\left| \frac{d\bar{P}_{ij}}{\bar{P}_{ij}} \right| = 0.033 + 0.033 = 0.066.$$

We assume, therefore, that the "standard deviation" of the probability distribution of the ratio  $\bar{P}_{ij}$  is 6.6 percent of its mean value.

A t-test was next performed to determine the 95 percent confidence interval around  $\bar{P}_{ij}$ . Because the number of samples,  $N=100$ , is large, we can approximate the t-distribution by the

TABLE 3. OFF-NORMAL CO-POLARIZED  $P_{ij}$  RATIOS OF SOILS INVESTIGATED

| Soil # | $P_{ij}$ ratio |          |          |          |          |          |
|--------|----------------|----------|----------|----------|----------|----------|
|        | $P_{21}$       | $P_{31}$ | $P_{41}$ | $P_{32}$ | $P_{42}$ | $P_{43}$ |
| 01     | 0.913          | 0.559    | 0.486    | 0.612    | 0.532    | 0.870    |
| 02     | 0.803          | 0.410    | 0.323    | 0.511    | 0.402    | 0.788    |
| 03     | 0.789          | 0.424    | 0.308    | 0.536    | 0.390    | 0.731    |
| 04     | 0.830          | 0.389    | 0.296    | 0.468    | 0.356    | 0.762    |
| 05     | 0.910          | 0.424    | 0.344    | 0.466    | 0.378    | 0.813    |
| 06     | 0.642          | 0.361    | 0.339    | 0.563    | 0.529    | 0.939    |
| 07     | 0.701          | 0.391    | 0.352    | 0.559    | 0.505    | 0.901    |
| 08     | 0.918          | 0.452    | 0.375    | 0.492    | 0.409    | 0.830    |
| 09     | 0.519          | 0.447    | 0.493    | 0.861    | 0.950    | 1.104    |
| 10     | 0.663          | 0.328    | 0.271    | 0.494    | 0.408    | 0.828    |
| 11     | 0.460          | 0.566    | 0.551    | 1.232    | 1.200    | 0.973    |
| 12     | 1.047          | 0.487    | 0.378    | 0.464    | 0.361    | 0.778    |
| 13     | 1.029          | 0.491    | 0.348    | 0.477    | 0.338    | 0.710    |
| 14     | 0.721          | 0.337    | 0.267    | 0.470    | 0.370    | 0.792    |
| 15     | 1.201          | 0.789    | 0.638    | 0.656    | 0.532    | 0.811    |
| 16     | 0.646          | 0.343    | 0.308    | 0.531    | 0.477    | 0.900    |
| 17     | 1.025          | 0.748    | 0.610    | 0.730    | 0.596    | 0.818    |
| 18     | 1.659          | 0.585    | 0.410    | 0.352    | 0.247    | 0.705    |



normal distribution (Mikhail, 1976). The 95 percent confidence interval on  $\overline{P}_{ij}$  is obtained from the statistical tables in Mikhail (1976) as  $\pm \frac{1.96d\overline{P}_{ij}}{\sqrt{N}}$ . This yields a 95 percent confidence interval of  $\pm 1.3$  percent around  $\overline{P}_{ij}$ . Thus, two  $\overline{P}_{ij}$  ratios are separable at a 95 percent confidence level if they differ by more than 1.3 percent of the larger ratio.

Based on the above criteria, all of the 18 soils investigated could be uniquely identified. The classification algorithm proceeds as follows. First, compute the  $\overline{P}_{21}$  ratio, which serves to classify 18, 15, 12, (13, 17), (01, 05, 08), (02, 03), 04, (06, 16), 10, 14, 07, 09, and 11. The soil numbers underlined have been uniquely identified based on the criteria discussed, while those within parentheses are indistinguishable among themselves, but identifiable from other soils. The  $\overline{P}_{31}$  ratio is then computed, based on which the remaining soils, i.e., 13, 17, 01, 05, 08, 02, 03, 06, and 16 are classified.

Thus, we infer that a three-wavelength laser reflectance system can be used to classify the benchmark soils considered here in this paper. In order to discriminate between a wider variety of geological and vegetative targets, Cvijin *et al.* (1987) suggest a four-wavelength ratio scheme.

### CONCLUSIONS

Based on our off-normal reflectance ratio classification algorithm, all of the 18 soils studied can be uniquely identified based on their mid-infrared reflectance structure. Off-normal co-polarized reflectance ratios have been shown to be relatively insensitive to variations in incidence angle, which demonstrates their suitability for soil discrimination over reflectance ratios computed for near-normal incidence. The work reported here can be used to augment various other terrain classification schemes.

### ACKNOWLEDGMENT

We acknowledge the assistance provided by Dr. L.N. Mielke, who furnished us the soil samples and participated in extensive technical discussion; Dr. M.A. Holmes, who helped analyze the soil mineralogy; P. Sink, who prepared the soils for X-ray diffraction analysis; and the two reviewers, whose enlightening comments served to improve this paper tremendously. The work was supported in part by the University of Nebraska Layman Fund and the U.S. Army Waterways Experiment Station through Battelle Delivery Order 2000.

### REFERENCES

Abramovitz, M., and I. Stegun, 1965. *Handbook of Mathematical Functions*, Dover, New York.

- Becker, F., P. Ramanantsizehena, and M. P. Stoll, 1985. Angular variation of the bidirectional reflectance of bare soils in the thermal infrared band, *Applied Optics*, Vol. 24, No. 3, pp. 365-375.
- Buol, S. W., F. D. Hole, and R. J. McCracken, 1989. *Soil Genesis and Classification*, Iowa State Univ. Press, Ames, Iowa.
- Clay, C. S., H. Medwin, and W. M. Wright, 1973. Specularly scattered sound and the probability density function of a rough surface, *Journal of the Acoustical Society of America*, Vol. 53, No. 6, pp. 1677-1682.
- Cvijin, P. V., D. Ignjatijevic, I. Mendas, I. Sreckovic, L. Pantani, and I. Pippi, 1987. Reflectance spectra of terrestrial surface materials at CO<sub>2</sub> laser wavelengths: effects on DIAL and geological remote sensing, *Applied Optics*, Vol. 26, No. 19, pp. 4323-4329.
- Dainty, J. C. 1984. "Introduction," Chapter 1, in *Laser Speckle and Related Phenomena*, (J. C. Dainty, Ed.), Springer-Verlag, Berlin.
- Donahue, R. L., R. W. Miller, and J. C. Shickluna, 1983. *Soils: An Introduction to Soils and Plant Growth*, Prentice-Hall; Englewood Cliffs, New Jersey.
- Eberhardt, J. E., J. G. Haub, and A. W. Pryor, 1985. Reflectivity of natural and powdered minerals at CO<sub>2</sub> laser wavelengths, *Applied Optics*, Vol. 26, No. 3, pp. 388-395.
- Fung, A. K., 1982. Review of random surface scatter models, *Proc. SPIE*, Vol. 358, Applications of Mathematics in Modern Optics, pp. 87-98.
- , 1984. Estimation of random surface parameters, *Electromagnetics*, Vol. 4, pp. 229-243.
- Leader, J. C., 1979. Analysis and prediction of laser scattering from rough-surface materials, *Journal of the Optical Society of America*, Vol. 69, No. 4, pp. 610-628.
- Mikhail, E. M., 1976. *Observations and Least Squares*, IEP, New York.
- Narayanan, R. M., S. E. Green, and D. R. Alexander, 1990. Mid-Infrared reflectance characteristics of selected benchmark soil samples, *Proc. USNC/URSI Meeting*, Boulder, Colorado, p. 98.
- Papoulis, A., 1984. *Probability, Random Variables and Stochastic Processes*, McGraw-Hill, New York.
- Salisbury, J. W., L. S. Walter and N. Vergo, 1987. *Mid-Infrared (2.1-25 μm) Spectra of Minerals: First Edition*, U.S. Geological Survey Open File Report 87-263.
- Shumate, M. S., S. Lundquist, U. Persson, and S. T. Eng, 1982. Differential reflectance of natural and man-made materials at CO<sub>2</sub> laser wavelengths, *Applied Optics*, Vol. 21, No. 13, pp. 2386-2389.
- Taylor, J. R., 1982. *An Introduction to Error Analysis*, University Science Books, Mill Valley, California.
- Willey, R. R., 1987. Results of a round-robin measurement of spectral emittance in the mid-infrared, *Proc. SPIE*, Vol. 807, The Hague, Netherlands.

(Received 27 August 1990; revised and accepted 15 April 1991)

## 1st Australian Conference on Mapping & Charting "Mapping for A Green Future" Adelaide, South Australia ♦ 14-17 September 1992

The Australian Institute of Cartographers is hosting a conference focusing on the role of cartography in monitoring and managing the nation's resources. Conference themes include:

Remote Sensing & Geographic Data for Environmental Management • Mapping Management & Professional Practice • Future Directions in Education & Training • Development of Mapping & Charting • International Mapping Opportunities • Thematic Cartography • GIS/LIS Development

For further information, contact: Conference Secretariat, 1st Australian Conference on Mapping and Charting  
GPP Box 1922, Adelaide, SOUTH AUSTRALIA